Case Study of a Prototypical Elementary Insertion Reaction: $C(^1D) + H_2 \rightarrow CH + H$

Shi Ying Lin and Hua Guo*

Department of Chemistry, University of New Mexico, Albuquerque, New Mexico 87131

Received: September 1, 2004

We present a thorough theoretical study of the title reaction using a wave packet based statistical model, which is ideally suited for reactions dominated by long-lived complexes. Both state-to-state integral cross sections and thermal rate constants were calculated for the three isotopic (H_2, D_2, and HD) reactions using a recent ab initio potential energy surface. Product (CH or CD) vibrational state distributions were found to decrease monotonically with the vibrational quantum number. The product rotational degree of freedom is highly excited up to the highest energetically available states, in good agreement with experimental results. For the C + HD reaction, the CD + H channel was found to be more populated than the CH + D channel, consistent with experimental observations. The thermal rate constants depend weakly on temperature and agree very well with recent experimental measurements at the room temperature.

I. Introduction

Recent years have witnessed a rapid increase of our knowledge on elementary chemical reactions, thanks to tremendous advances in both experimental[1,2] and theoretical fronts.[3−6] Direct comparison between experimentally measured and quantum mechanically calculated state-resolved scattering observables has become possible for many triatomic and some tetratomic systems. In particular, significant progress has been made in understanding direct activated atom−diatom abstraction reactions, such as the H + H_2 and F + H_2 reactions. As a result, attention has recently begun to shift to insertion reactions,[7−14] in which the potential energy surfaces are often dominated by deep wells rather than barriers. Examples of such elementary reactions include those between electronically excited atoms, such as $O(^1D)$, $C(^1D)$, $S(^1D)$, and $N(^2D)$, and H_2 in its ground electronic state. As compared with abstraction reactions, the dynamics of insertion reactions is more complex and more challenging for a quantum mechanical characterization because of the large number of quantum states supported by the deep well and the long lifetime of the resonance states.

It is perhaps worthwhile to compare the title reaction (R1) with the most extensively studied prototype (R2) for insertion reactions:

$$C(^1D) + H_2(X^1\Sigma_g^+) \rightarrow CH(X^2\Pi) + H(^2S) \qquad \Delta H_0 = -6.3 \text{ kcal/mol} \quad \text{(R1)}$$

$$O(^1D) + H_2(X^1\Sigma_g^+) \rightarrow OH(X^2\Pi) + H(^2S) \qquad \Delta H_0 = -43.4 \text{ kcal/mol} \quad \text{(R2)}$$

Like other members of the insertion reaction family, both are dominated by potential energy surfaces featuring deep wells connecting without a barrier to the reactant and product channels. However, R1 has a number of remarkable features. First, it is believed to proceed on the lowest-lying singlet (a^1A_1) electronic state,[15] which has a relatively high abstraction barrier at linearity of 12.35 kcal/mol.[16] As a result, the adiabatic abstraction mechanism is unlikely to operate at low temperatures. Second, unlike R2,[17−19] the involvement of nonadiabatic abstraction channels in R1 is minimal. The existence of the b^1B_1 state, which forms the Renner−Teller pair with the a^1A_1 state at linearity, does not qualitatively change the picture as both states correlate with the same reactant and product channels in R1. As a result, R1 is considered as a clean insertion reaction,[12] without involvement of abstraction pathways. In addition, R1 is much less exothermic than R2, rendering the intermediate CH_2 complex rather long-lived, which justifies a statistical treatment.[20,21] In many respects, R1 strongly resembles the $S(^1D)$ + H_2 reaction.[22−25]

From a practical perspective, R1 has important implications in organic chemistry, particularly in understanding the mechanisms of a large number of carbon−alkane reactions involving the insertion of the carbon atom into C−H or C−C σ bonds.[26,27] It may also play an important role in combustion reactions,[28] gasification of coal,[29] and astrochemistry.[30] For these reasons, the title reaction has attracted much experimental attention,[31−39] including recent crossed molecular beam experiments.[12,13] In addition, the intermediate of the reaction, namely, methylene, is itself the simplest carbene, which is known to have some intriguing spectroscopic[40] and chemical properties.[41] Theoretically, CH_2 contains only eight electrons and is thus amenable to high level ab initio calculations of its potential energy surfaces.[42−47] Indeed, a highly accurate global potential energy surface of the a^1A_1 state has been reported by Bussery-Honvault et al.[16]

The availability of the high quality potential energy surface has stimulated several dynamical studies of the reaction. Launay and co-workers[16,48] carried out impressive time-independent quantum and quasi-classical trajectory calculations of both integral and differential cross sections using the original version of the potential energy surface.[16] Later, wave packet studies were reported by the current authors,[49−51] using a slightly modified potential energy surface.[52] The reaction probabilities obtained from both quantum mechanical calculations are strongly oscillatory, indicative of the participation of long-lived resonance states. Integral and differential cross sections obtained

* Corresponding author. Phone: (505) 277-1716. Fax: (505) 277-2609. E-mail: hguo@unm.edu.

10.1021/jp046039y CCC: $27.50
Published on Web 10/26/2004

by the time-independent quantum method at a single energy point (7.8 kJ/mol)[48] are in general agreement with the quasi-classical trajectory results[13,48,52] and consistent with available experimental data.[12,13] Agreement between measured and calculated rate constants from the wave packet approach is less satisfactory, presumably because of the dynamic approximations used in the calculation.[50] Very recently, isotopic effects of the reaction were explored using the same wave packet method.[51]

Despite the aforementioned advances, our understanding of the title reaction is far from complete. Although the time-independent quantum mechanical method of Launay et al.[16,48] is free of dynamic approximations, information on the energy dependence of the cross sections, which is needed to determine the rate constant, can be very expensive to obtain. On the other hand, wave packet approaches,[49−51] which yield scattering attributes at all energies, suffer from large grids and long propagation because of the large number of quantum states supported by the deep potential well. This problem is particularly acute for the title reaction because the resonance states typically have lifetimes on the order of a few picoseconds. To make the computation feasible, simplifications such as the capture model[53,54] or the centrifugal sudden[55]/coupled state[56] (CS) approximation were used. Compounding the difficulties, the commonly used CS approximation was found to cause significant errors for such complex-forming reactions.[50,57] Although the quasi-classical trajectory method yields important information with relatively low computational costs,[13,48,52] the results may be plagued by the neglect of quantum effects such as zero-point energy and tunneling. These difficulties have until now prevented us from an accurate and consistent understanding of this important reaction.

Paradoxically, the dominance of many closely spaced long-lived resonances in complex-forming reactions such as R1, which has proven detrimental to exact wave packet based approaches due to the combined effect of a large grid and long propagation, offers a simple and rather accurate alternative for treating such reactions. Indeed, it has been realized for some time now that the long lifetime of the reaction intermediate (e.g., the metastable CH_2 complex in the title reaction) allows a separate and statistical treatment of the formation and decay of the complex.[58−61] It has been shown by Manolopoulos and co-workers[20,21] and more recently by us[62] that an improved statistical model is capable of reproducing nearly quantitatively exact quantum mechanical integral, and more impressively, differential cross sections for a number of complex-forming reactions, at a fraction of the cost. The title reaction is especially well-suited for a statistical treatment because the resonance lifetimes are known to be very long, thanks to the deep well and small exothermicity. The statistical nature of the reaction is also supported by overwhelming experimental evidence, such as the backward−forward symmetry in the product angular distribution[12,13] and near statistical product distributions.[33,35−37,39]

Encouraged by the remarkable performance of the improved statistical model, we report here a thorough investigation of the title reaction and its isotopic counterparts using the recently proposed wave packet based statistical method,[62] which promises a consistent and accurate characterization of the reaction dynamics. To this end, state-to-state integral cross sections and rate constants are obtained for the title reaction involving three different isotopomers of H_2. Some preliminary results have already been reported in a recent communication.[62] This paper is organized as follows. In the next section, the relevant theoretical methods and their numerical implementations are briefly outlined. In Section III, the calculated results are presented and discussed. Finally, in Section IV, conclusions are made.

II. Methods

In the statistical model, the formation and decay of the long-lived complex in the reaction are treated as separate events. This is expected to be valid if the lifetime of the complex is sufficiently long. In addition, the population of open channels is completely statistical, namely, determined by availability. The statistical argument is similar in spirit to the RRKM theory for unimolecular reactions.[63] Thus, the state-to-state reaction probability $p_{f\leftarrow i}(E)$ is given by a product of the capture probability in the reactant (i) channel and the fraction of population decaying to the product (f) channel:[59,61]

$$p_{f\leftarrow i}(E) = p_i^{(c)}(E) \times \frac{p_f^{(c)}(E)}{\sum_l p_l^{(c)}(E)} \qquad (1)$$

where $p_l^{(c)}(E)$ represents the probability of being captured by the deep well for a particular channel (l). The summation in the denominator of eq 1 runs over all the open channels at energy E. It is obvious that detailed balance is maintained in eq 1. The diagonal indices, such as the total angular momentum J and parity, have been suppressed in eq 1. Once the state-to-state probabilities for all J are known, many experimentally measurable quantities, such as the integral cross section, thermal rate constant, and product state distributions, can be calculated in a straightforward fashion. Differential cross sections can also be obtained by using a random phase approximation,[21] but they contain limited information because of the guaranteed backward−forward symmetry.

Although the capture probabilities can be estimated from model long-range potentials, their explicit calculation in a realistic potential energy surface can drastically improve the accuracy of the statistical model, as shown by Manolopoulos and co-workers.[20,21] This is particularly important for the title reaction because both zero-point energy and tunneling through the centrifugal barrier are substantial. Technically, the capture probabilities can be computed with ease using either the coupled-channel[20,21] or wave packet approach.[62] The latter is energy global, which is advantageous if energy dependence is of interest. As compared with exact methods, the statistical approach is very efficient because these inelastic scattering-like calculations can be carried out in specific arrangement channels with small grids/bases and short propagation. This approach thus avoids a common problem in reactive scattering calculations, namely, choosing and/or changing coordinate systems. In addition, the CS approximation has been shown to perform quite well, again because the dynamics is dominated by long-range interactions.

In this work, we computed capture probabilities using the wave packet based method proposed earlier.[62] Since the details of the method can be found in the original work, we provide here only a brief review. In short, the capture probability ($p_l^{(c)}$) is calculated in a specific arrangement channel by computing the flux of an incoming wave packet. The (real) wave packet was propagated using the modified Chebyshev propagator[64] with damping terms in both asymptotic and complex-forming regions, as illustrated in Figure 1. These damping terms, in analogy to the absorption boundary conditions, were designed to remove the outgoing wave packet in the asymptote and that entering the complex-forming region of the potential energy surface. The

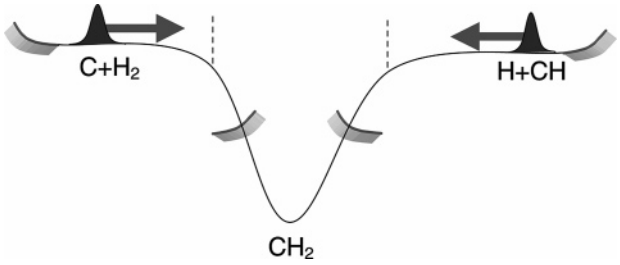

Figure 1. Illustration of the wave packet based method for calculating capture probabilities for the $C + H_2 \rightarrow CH + H$ reaction. The flux for entering the complex region is calculated at the dashed lines before the wave packet is absorbed by the damping boundary conditions (shaded regions).

capture probability was obtained from the energy-resolved flux[49,65] calculated at the gate of the complex-forming region from a specific channel, represented by vertical dashed lines in Figure 1. The calculation was repeated for all open channels and for all necessary total angular momentum quantum numbers and parities. Typically, each wave packet propagation requires less than 1 min on a regular workstation.

III. Results and Discussion

IIIA. Calculation Details. We employed the corresponding Jacobi coordinates (R,r,γ) in each arrangement channels to calculate capture probabilities. Here, r and R are the diatomic internuclear distance and the distance between the atom and the center of mass of the diatom, respectively, and γ is the Jacobi angle. The spin of the diatomic product was ignored, and the $j = N$ approximation was imposed because of the dominance of the highly excited rotational states (*vida infra*). The Hamiltonian was discretized in a mixed direct product representation. For R and r, a discrete variable representation (DVR)[66] is used while a finite basis set representation (FBR) is used for angular dimension. For R, an equidistant grid was defined in $[R_{min},R_{max}]$ as $R_{\alpha_1} = R_{min} + \alpha_1(R_{max} - R_{min})/(N_R + 1)$ with $\alpha_1 = 1, 2, ..., N_R$, which facilitates a fast sine Fourier transform between the DVR and FBR.[67] The number of grid points depends on the specific arrangement channel. For r, on the other hand, a potential optimized DVR[68] was used, which substantially decreased the number of grid points. For the title system, two to three points were often sufficient to converge the results. For the angular dimension, associated Legendre functions were chosen as the basis. A pseudo-spectral transformation was used to transform the wave packet between the DVR and FBR. Finally, the permutation symmetry was adapted for the $C + H_2$ (D_2) channels, which separates the even and odd j states of H_2 (D_2) and halves the angular grid. However, such symmetry adaptation is not possible for other arrangement channels. Other details of the calculation can be found in our previous publications.[49−51]

IIIB. Capture Probabilities. As shown in previous work,[20,21] the CS approximation that ignores the Coriolis coupling is a reasonable approximation in calculating the capture probabilities. To verify this conclusion, we have compared in Figure 2 the capture probability for the $C + H_2$ ($v_i = 0$, $j_i = 0$) channel at several J values. It is clear that the CS results follow closely with the exact probabilities. Similar behaviors were observed in the CH + H channel. The differences at large J values are small and not expected to significantly alter the final results. The accuracy of the CS approximation can be readily understood since the centrifugal barrier is located at relatively large atom−diatom distances where the helicity quantum number (Ω) is often well-conserved. The results reported next were thus obtained with the CS Hamiltonian. We have also tested several capture absorbing boundaries and found no substantial changes in the capture probability.

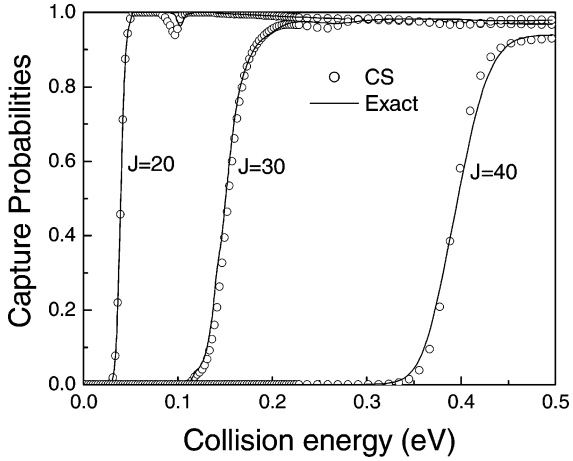

Figure 2. Comparison of capture probabilities obtained from the exact (lines) and the approximate CS (circles) methods.

It is interesting to note that the capture probabilities in the figures have little oscillation, in sharp contrast to the reaction probabilities obtained from exact quantum calculations.[16,49] The absence of oscillation is a direct consequence of damping of the incoming wave packet in the complex region. As a result, the reaction probabilities obtained from the capture probabilities are averaged over these resonance structures and thus inaccurate.[21] Nevertheless, the statistical model is expected to produce accurate cross sections since the oscillatory structure is washed out when the reaction probabilities are summed over the total angular momentum. We also note that the capture probabilities have sharp thresholds, which are primarily determined by the centrifugal barrier. Very little backscattering is observed as the wave packet is almost completely captured above the thresholds. Figure 2 also suggests that a J-shifting model[69] might work very well.

IIIC. Total Integral Cross Sections and Thermal Rate Constants. The upper panel of Figure 3 displays the total integral cross sections for the title reaction with three hydrogen isotopomers in their ground ro-vibrational states. Interestingly, the cross sections are very similar and show little isotopic variation. The lack of isotope dependence in total cross sections has been observed before in other insertion reactions,[23,70] but its origin is not yet clear. The cross sections all feature a sharp decrease at low energies and leveling off at higher energies, a signature of barrierless insertion reactions. The accuracy of the statistical model is evidenced by the excellent agreement (31.8 vs 30.5 Å^2) with the only existing exact quantum mechanical total cross section for the $C + H_2$ reaction at the collision energy of 7.8 kJ/mol.[48] On the contrary, the total cross sections computed earlier using the capture model and CS approximation (23.8 and 15.5 Å^2)[50] are significantly lower than the exact value, underscoring the deficiency of those models. The cross section was also found to depend weakly on the initial rotational excitation of the diatomic reactant. For the $C + H_2$ reaction, for example, the total integral cross section at 3.7 kJ/mol is 40.8, 40.0, 38.9, and 38.1 Å^2 for $j_i = 0$, 1, 2, and 3, respectively. The decrease of the total cross section with respect to the rotational excitation is consistent with the insertion mechanism.

By Boltzmann averaging of the total integral cross sections over the kinetic energy and initial rotational states, thermal rate constants for the three isotopic variants were obtained and displayed in the lower panel of the same figure. All the rate

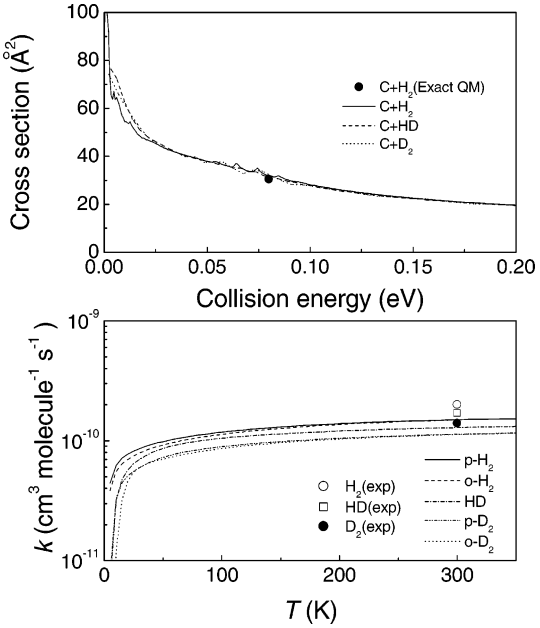

Figure 3. Upper panel: dependence of total integral cross sections on the collision energy for the three isotopic reactions. The exact quantum mechanical result[48] at 0.080 eV (7.8 kJ/mol) is also included. Lower panel: temperature dependence of thermal rate constants for C + *p*-H_2 (solid line), C + *o*-H_2 (dashed line), C + HD (dash−dotted line), C + *p*-D_2 (dash−dot−dotted line), and C + *o*-D_2 (dotted line). The recent experimental thermal rate constants[39] for C + H_2 (open circle), C + HD (open square), and C + D_2 (closed circle) at room temperature are also shown for comparison (for visual clarity, the experimental error bars are not included).

constants show similar temperature dependence characteristic of a barrierless reaction. After a rapid rise at very low temperatures, they increase slowly with the temperature. For the C + H_2 and C + D_2 reactions, the rate constants for para-hydrogen is slightly larger than that for ortho-hydrogen at low temperatures, while the differences diminish as the temperature increases.

As shown in Figure 3, the rate constants at the room temperature are in excellent agreement with the recent experimental measurements.[39] Except for the rate constant of the C + HD reaction, which is slightly smaller than the lower bound of experimental error bar, other two rate constants are well within the experimental error ranges. In particular, the calculated rate constants at 300 K are 1.50×10^{-10}, 1.29×10^{-10}, and 1.13×10^{-10} cm^3 molecule^{-1} s^{-1} for H_2, HD, and D_2, respectively, while the corresponding experimental values are $(2.0 \pm 0.6) \times 10^{-10}$, $(1.7 \pm 0.4) \times 10^{-10}$, and $(1.4 \pm 0.3) \times 10^{-10}$ cm^3 molecule^{-1} s^{-1}. The results reported here represent a much better agreement with experiment than our previous study,[50] which used either the CS approximation or a capture model. In addition, they are in exactly the same order as the experimental results (i.e., $k_{H_2} > k_{HD} > k_{D_2}$), a trend not well-reproduced in our earlier theoretical work. Since the cross sections are nearly identical, this ordering of rate constants for the three isotope reactions is largely a kinematic effect determined by the square root of the reduced mass.

IIID. CD/CH Branching Ratio in C + HD Reaction. The C + HD reaction produces two distinguishable product channels, namely, CH + D and CD + H. The branching ratio between the two channels should be a sensitive probe of the reaction dynamics.[70] The latest experimentally measured CD/CH branching ratio at 3.7 kJ/mol is 1.6 ± 0.1.[39] The calculated branching ratios for several initial HD rotational states are displayed in Figure 4, which clearly show the dominance of the CD + H

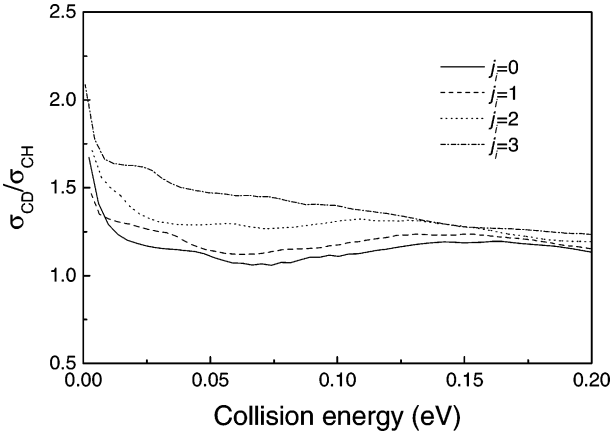

Figure 4. Energy dependence of the CD/CH branching ratio of the C + HD reaction for different rotational states of HD.

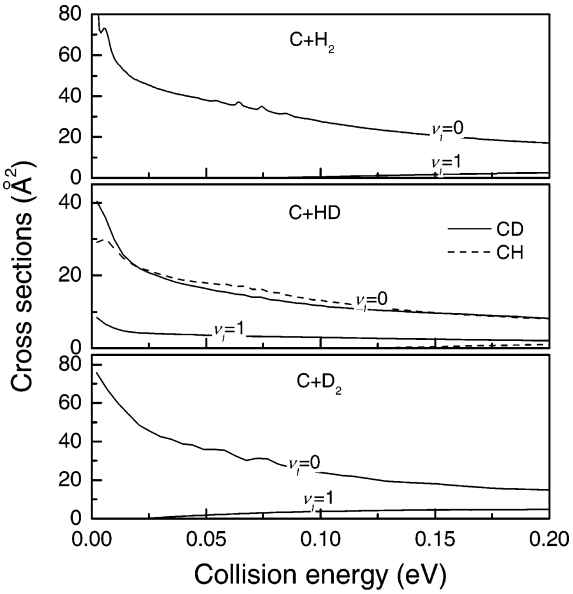

Figure 5. Product vibrational state distributions as a function of collision energy for three isotopic reactions.

channel at all collision energies below 0.2 eV. This can be readily understood from a statistical point of view as CD possesses more open channels than CH, due to the difference in the reduced masses. Similar observations have been made in other theoretical studies of insertion reactions such as O(^1D) + HD and S(^1D) + HD.[71−73]

Quantitatively, the calculated CD/CH ratio at the experimental energy of 3.7 kJ/mol (0.038 eV) is 1.2 for the rotationless ($j_i = 0$) HD state but increases if rotationally excited states of HD are considered. The agreement with experimental data[35,39] is reasonable but not perfect. It is not clear at this moment what factors are responsible for the discrepancy, and further theoretical and experimental investigations will certainly be welcome. In our previous study[51] where a capture model was used based on $J = 0$ quantum reaction probabilities, a branching ratio of 1.7 was reported. However, the excellent agreement with experiment may be fortuitous because of the large errors introduced by the capture model.

IIIE. Product Vibrational State Distributions. More detailed information about the reaction dynamics can be obtained from state-resolved quantities. In Figure 5, the vibrational state resolved cross sections are plotted against the collision energy for all three isotopic reactions. For clarity, only results from the ground ro-vibrational state of the diatomic reactants (H_2,

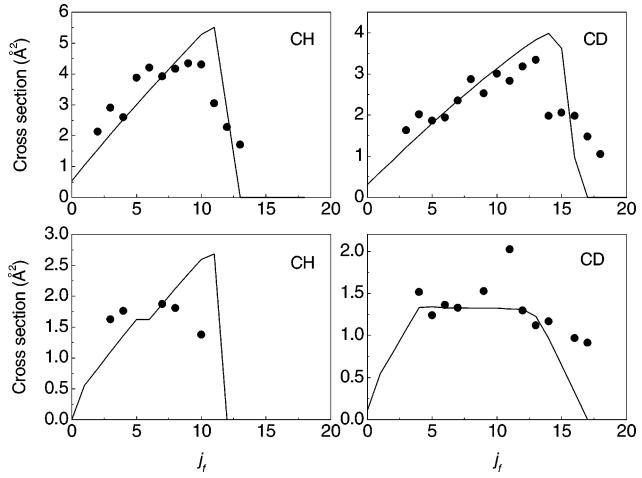

Figure 6. Product rotational distributions in the $v_f = 0$ manifold at the collision energy of 3.7 kJ/mol for the C + H_2/D_2 (upper panels) and C + HD (lower panels) reactions. The experimental results,[39] represented by cycles, were normalized with the theoretical ones at $j_f = 7$.

D_2, and HD) are presented. As compared with abstraction reactions in which inverted vibrational state distributions are common, insertion reactions often produce less vibrational excitation in the product because of the nonlinear reaction path. This is certainly true for the title reaction and other insertion reactions dominated by long-lived intermediates, such as S(^1D) + H_2.[24,25] As shown in Figure 5, all the diatomic products are dominated by the ground vibrational states. The $v_f = 1$ state in the CD + H channel is open even at zero kinetic energy and has much larger population than other diatoms. Also shown in the figure, vibrational excitation in the products increases somewhat with the collision energy. This picture is consistent with the experimental observations of very limited vibrational excitation in the product[35,37,39] and with previous theoretical investigations.[16,48,51,52] Specifically for the C + H_2 ($j_i = 0$) reaction, the $v_f = 1/v_f = 0$ ratio is 0.0035 and 0.11 at 7.8 and 16.0 kJ/mol, respectively. The initial rotational excitation seems to enhance the vibrational excitation in the product. The $v_f = 1/v_f = 0$ ratio is 0.016 and 0.13 at 7.8 and 16.0 kJ/mol, respectively, for the C + H_2 ($j_i = 1$) reaction. These observations are consistent with the latest experimental and theoretical results.[13]

IIIF. Product Rotational State Distributions. In contrast to the relatively low product vibrational excitation, insertion reactions are capable of generating highly inverted product rotational state distributions. This is because the products are statistically formed from the highly bending excited intermediate complex. In Figure 6, the calculated product rotational state distributions from reactions with the ground ro-vibrational state reactants at the collision energy of 3.7 kJ/mol (0.038 eV) are compared with the recent experimental measurements.[39] Since the population in the excited vibrational state is generally small at this energy, only results in the $v_f = 0$ vibrational manifold are presented. The theoretical distributions typically increase smoothly with the rotational quantum number and then decrease abruptly near the highest allowed rotational states. To facilitate the comparison with theoretical results, the experimental distributions were normalized at $j_f = 7$ corresponding to theoretical population. Unfortunately, not all the rotational states were resolved in the experiment,[39] but the trend is clearly descendible.

The general agreement between theory and experiment is quite reasonable. As expected, all isotopic reactions produce

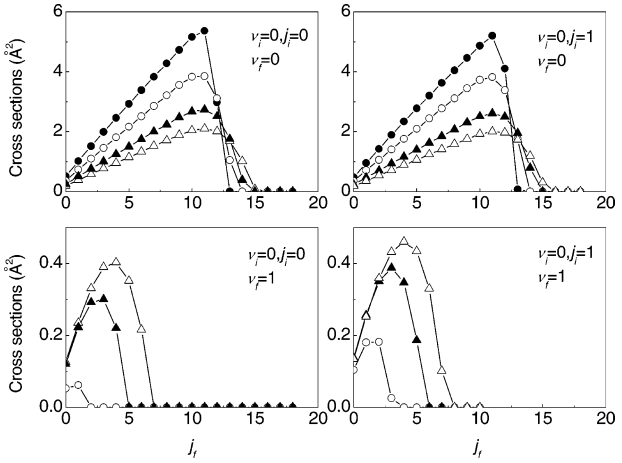

Figure 7. Product rotational state distributions of the C + H_2 reaction in $v_f = 0$ manifold (upper panel) and $v_f = 1$ (lower panel) at collision energies of 4.0 (●), 7.8 (○), 12.0 (▲), and 16.0 kJ/mol (△).

highly excited rotational state distributions extending to the highest possible rotational states. In both the C + H_2 and C + D_2 reactions, the nearly quantitative agreement with the experimental distributions are quite remarkable. The CD distribution extends to larger rotational quantum numbers, due to its smaller rotational constant and thus larger number of open channels. In the C + HD reaction, the CD distribution is also broader. The agreement should be viewed in the context of considerable uncertainties associated with the experimental conditions,[39] in which the initial state distribution of the reactant and the collision energy are not well-characterized.

The energy dependence of the product rotational state distributions is similar among all isotopic systems. As a representative, we selected the C + H_2 reaction as an example. The rotational state distributions of CH ($v_f = 0$ and 1) are displayed in the upper and lower panels of Figure 7 at several collision energies for two initial rotational states of H_2 ($j_i = 0$ and 1). As the energy increases, as a general rule, the distributions become broader and more highly excited. This observation is again consistent with the statistical nature of the reaction. We note that two of the collision energies, 7.8 and 16.0 kJ/mol, are the same as the experimental energies in a recent crossed molecular beam study,[13] which unfortunately did not report rotational state resolution.

IV. Conclusions

In this work, we present a systematic and detailed study of the elementary insertion reactions of C(^1D) with H_2 and its deuterated isotopomers using an ab initio based global potential energy surface. The calculated reaction attributes range from thermal rate constants, total cross sections, product state distributions, to the CD/CH branching ratio. The uniqueness of this work is that it provides a consistent quantum mechanical characterization of this important elementary reaction with uniform accuracy. The knowledge acquired in studies such as this can be very useful in understanding other reactions that proceed with similar mechanisms.

In particular, the calculated total integral cross sections are all monotonically decay functions of the collision energy, in keeping with the barrierless insertion mechanism. The theoretical thermal rate constants show weak temperature dependence and excellent agreement with measured experimental data at the room temperature. The rate constants for three isotopic reactions were found to have the same order as that observed in the experiment: $k_{H_2} > k_{HD} > k_{D_2}$. Despite the isotopic variations

in the thermal rate constants, the total cross sections are almost identical for the three isotopic reactions at all collision energies. As a result, the isotope effect in the rate constants is purely kinematic.

The diatomic products of the title reaction were found to have limited vibrational excitation but very hot and inverted rotational state distributions. The good agreement with limited experimental data confirms the statistical nature of the reaction. In addition, the CD + H channel was found to be more populous than the CH + D channel in the C + HD reaction. Again, this signifies the statistical nature of the reaction as the former possesses more open channels.

Despite its approximate nature, the statistical model used in this work to characterize the reaction dynamics has been shown to be nearly quantitatively accurate for reactions dominated by long-lived complexes. The approximations in this statistical model are apparently much less severe for the title reaction than several dynamical approximations previously used to estimate cross-sections. The wave packet based implementation of the statistical model has the particular advantage of providing a uniformly accurate set of scattering attributes ranging from the thermal rate constant to state-to-state cross sections. In light of the current computational difficulties in characterization of complex-forming reactions, the current approach represents an efficient quantum mechanical alternative to other theoretical methods. This is particularly true for complex-forming reactions involving more than three atoms.

Acknowledgment. This work was supported by the National Science Foundation (CHE-0348858). We thank David Manolopoulos and Ed Rackham for many useful discussions on the statistical model.

References and Notes

(1) Casavecchia, P. *Rep. Prog. Phys.* **2000**, *63*, 355.
(2) Liu, K. *Annu. Rev. Phys. Chem.* **2001**, *52*, 139.
(3) Bowman, J. M.; Schatz, G. C. *Annu. Rev. Phys. Chem.* **1995**, *46*, 169.
(4) Zhang, J. Z. H. *Theory and Application of Quantum Molecular Dynamics*; World Scientific: Singapore, 1999.
(5) Nyman, G.; Yu, H.-G. *Rep. Prog. Phys.* **2000**, *63*, 1001.
(6) Althorpe, S. C.; Clary, D. C. *Annu. Rev. Phys. Chem.* **2003**, *54*, 493.
(7) Alexander, A. J.; Blunt, D. A.; Brouard, M.; Simons, J. P.; Aoiz, F. J.; Banares, L.; Fujimura, Y.; Tsubouchi, M. *Faraday Discuss*. **1997**, *108*, 375.
(8) Alagia, M.; Balucani, N.; Cartechini, L.; Casavecchia, P.; Kleef, E. H. V.; Volpi, G.G.; Kuntz, P. J.; Sloan, J. J. *J. Chem. Phys.* **1998**, *108*, 6698.
(9) Liu, X.; Lin, J. J.; Harich, S.; Schatz, G. C.; Yang, X. *Science* **2000**, *289*, 1536.
(10) Gray, S. K.; Balint-Kurti, G. G.; Schatz, G. C.; Lin, J. J.; Liu, X.; Harich, S.; Yang, X. *J. Chem. Phys.* **2000**, *113*, 7330.
(11) Aoiz, F. J.; Banares, L.; Castillo, J. F.; Brouard, M.; Denzer, W.; Vallance, C.; Honvault, P.; Launay, J.-M.; Dobbyn, A. J.; Knowles, P. J. *Phys. Rev. Lett.* **2001**, *86*, 1729.
(12) Bergeat, A.; Cartechini, L.; Balucani, N.; Capozza, G.; Philips, L. F.; Casavecchia, P.; Volpi, G. G.; Bonnet, L.; Rayez, J.-C. *Chem. Phys. Lett.* **2000**, *327*, 197.
(13) Balucani, N.; Capozza, G.; Cartechini, L.; Bergeat, A.; Bobbenkamp, R.; Casavecchia, P.; Aoiz, F. J.; Banares, L.; Honvault, P.; Bussery-Honvault, B.; Launay, J.-M. *Phys. Chem. Chem. Phys*. **2004**, in press.
(14) Balucani, N.; Cartechini, L.; Capozza, G.; Segoloni, E.; Casavecchia, P.; Volpi, G. G.; Aoiz, F. J.; Banares, L.; Honvault, P.; Launay, J.-M. *Phys. Rev. Lett.* **2002**, *89*, 013201.
(15) Bearda, R. A.; vanHemert, M. C.; vanDishoeck, E. F. *J. Chem. Phys.* **1992**, *97*, 8240.
(16) Bussery-Honvault, B.; Honvault, P.; Launay, J.-M. *J. Chem. Phys.* **2001**, *115*, 10701.
(17) Ho, T.-S.; Hollebeek, T.; Rabitz, H.; Harding, L. B.; Schatz, G. C. *J. Chem. Phys.* **1996**, *105*, 10472.
(18) Drukker, K.; Schatz, G. C. *J. Chem. Phys.* **1999**, *111*, 2451.
(19) Gray, S. K.; Petrongolo, C.; Drukker, K.; Schatz, G. C. *J. Phys. Chem.* **1999**, *103*, 9448.
(20) Rackham, E. J.; Huarte-Larranaga, F.; Manolopoulos, D. E. *Chem. Phys. Lett.* **2001**, *343*, 356.
(21) Rackham, E. J.; Gonzalez-Lezana, T.; Manolopoulos, D. E. *J. Chem. Phys.* **2003**, *119*, 12895.
(22) Lee, S.-H.; Liu, K. *J. Phys. Chem.* **1998**, *A102*, 8637.
(23) Zyubin, A. S.; Mebel, A. M.; Chao, S. D.; Skodje, R. T. *J. Chem. Phys.* **2001**, *114*, 320.
(24) Honvault, P.; Launay, J.-M. *Chem. Phys. Lett.* **2003**, *370*, 371.
(25) Banares, L.; Aoiz, F. J.; Honvault, P.; Launay, J.-M. *J. Phys. Chem.* **2004**, *A108*, 1616.
(26) Wolf, A. P. *Adv. Phys. Org. Chem.* **1964**, *2*, 202.
(27) Skell, P. S.; Havel, J. J.; McGlinchey, M. J. *Acc. Chem. Res.* **1973**, *6*, 97.
(28) Gaydon, A. G. *The Spectroscopy of Flames*; Chapman and Hall: London, 1974.
(29) Williams, A.; Pourkashanian, M.; Skorupska, N. *Combustion and Gasification of Coal*; Taylor and Francis: New York, 2000.
(30) Flower, D. R.; PineaudesForets, G. *Mon. Not. R. Astron. Soc.* **1998**, *297*, 1182.
(31) Braun, W.; Bass, A. M.; Davis, D. D.; Simmons, J. D. *Proc. Royal Soc. (London)* **1969**, *A312*, 417.
(32) Husain, D.; Kirsch, L. J. *Chem. Phys. Lett.* **1971**, *9*, 412.
(33) Jursich, G. M.; Wiesenfeld, J. R. *Chem. Phys. Lett.* **1984**, *110*, 14.
(34) Jursich, G. M.; Wiesenfeld, J. R. *J. Chem. Phys.* **1985**, *83*, 910.
(35) Fisher, W. H.; Carrington, T.; Sadowski, C. M.; Dugan, C. H. *Chem. Phys.* **1985**, *97*, 433.
(36) Scott, D. C.; deJuan, J.; Robie, D. C.; Schwartz-Lavi, D.; Reisler, H. *J. Phys. Chem.* **1992**, *96*, 2509.
(37) Mikulecky, K.; Gericke, K.-H. *J. Chem. Phys.* **1993**, *98*, 1244.
(38) Mikulecky, K.; Gericke, K.-H. *Chem. Phys.* **1993**, *175*, 13.
(39) Sato, K.; Ishida, N.; Kurakata, T.; Iwasaki, A.; Tsuneyuki, S. *Chem. Phys. Lett.* **1998**, *237*, 195.
(40) Schaefer, H. F. *Science* **1986**, *231*, 1100.
(41) Moss, R. A.; Jones, M. *Carbenes*; Wiley: New York, 1975.
(42) Blint, R. J.; Newton, M. D. *Chem. Phys. Lett.* **1975**, *32*, 178.
(43) Whitlock, P. A.; Muckerman, J. T.; Kroger, P. M. In *Potential Energy Surfaces and Dynamical Calculations*; Truhlar, D. G., Ed.; Plenum: New York, 1981.
(44) Knowles, P. J.; Handy, N. C.; Carter, S. *Mol. Phys.* **1983**, *49*, 681.
(45) Comeau, D. C.; Shavitt, I.; Jensen, P.; Bunker, P. R. *J. Chem. Phys.* **1989**, *90*, 6491.
(46) Green, W. H.; Handy, N. C.; Knowles, P. J.; Carter, S. *J. Chem. Phys.* **1991**, *94*, 118.
(47) Harding, L. B.; Guadagnini, R.; Schatz, G. C. *J. Phys. Chem.* **1993**, *97*, 5472.
(48) Banares, L.; Aoiz, F. J.; Honvault, P.; Bussery-Honvault, B.; Launay, J.-M. *J. Chem. Phys.* **2003**, *118*, 565.
(49) Lin, S. Y.; Guo, H. *J. Chem. Phys.* **2003**, *119*, 11602.
(50) Lin, S. Y.; Guo, H. *J. Phys. Chem.* **2004**, *A108*, 2141.
(51) Lin, S. Y.; Guo, H. *J. Chem. Phys.* **2004**, *121*, 1285.
(52) Banares, L.; Aoiz, F. J.; Vazquez, S. A.; Ho, T.-S.; Rabitz, H. *Chem. Phys. Lett.* **2003**, *374*, 243.
(53) Clary, D. C.; Henshaw, J. P. *Faraday Discuss.* **1987**, *84*, 333.
(54) Gray, S. K.; Goldfield, E. M.; Schatz, G. C.; Balint-Kurti, G. G. *Phys. Chem. Chem. Phys.* **1999**, *1*, 1141.
(55) Pack, R. T. *J. Chem. Phys.* **1974**, *60*, 633.
(56) McGuire, P.; Kouri, D. J. *J. Chem. Phys.* **1974**, *60*, 2488.
(57) Meijer, A. J. H. M.; Goldfield, E. M. *J. Chem. Phys.* **1999**, *110*, 870.
(58) Light, J. C. *J. Chem. Phys.* **1964**, *40*, 3221.
(59) Pechukas, P.; Light, J. C. *J. Chem. Phys.* **1965**, *42*, 3281.
(60) Pechukas, P.; Light, J. C.; Rankin, C. *J. Chem. Phys.* **1966**, *44*, 794.
(61) Miller, W. H. *J. Chem. Phys.* **1970**, *52*, 543.
(62) Lin, S. Y.; Guo, H. *J. Chem. Phys.* **2004**, *120*, 9907.
(63) Marcus, R. A.; Rice, O. K. *J. Phys. Colloid Chem.* **1951**, *55*, 894.
(64) Chen, R.; Guo, H. *Comput. Phys. Comm.* **1999**, *119*, 19.
(65) Meijer, A. J. H. M.; Goldfield, E. M.; Gray, S. K.; Balint-Kurti, G. G. *Chem. Phys. Lett.* **1998**, *293*, 270.
(66) Light, J. C.; Carrington, T. *Adv. Chem. Phys.* **2000**, *114*, 263.
(67) Kosloff, D.; Kosloff, R. *J. Comput. Phys.* **1983**, *52*, 35.
(68) Echave, J.; Clary, D. C. *Chem. Phys. Lett.* **1992**, *190*, 225.
(69) Bittererova, M.; Bowman, J. M.; Peterson, K. *J. Chem. Phys.* **2000**, *113*, 6186.
(70) Fitzcharles, M. S.; Schatz, G. C. *J. Phys. Chem.* **1986**, *90*, 3634.
(71) Hankel, M.; Balint-Kurti, G. G.; Gray, S. K. *J. Phys. Chem.* **2001**, *105*, 2330.
(72) Chang, A. H. H.; Lin, S. H. *Chem. Phys. Lett.* **2000**, *320*, 161.
(73) Chao, S. D.; Skodje, R. T. *J. Phys. Chem.* **2001**, *A105*, 2474.